

An inverse radiation problem

C.-H. HO and M. N. ÖZİŞİK

Department of Mechanical and Aerospace Engineering, North Carolina State University,
 Box 7910, Raleigh, NC 27695-7910, U.S.A.

(Received 3 December 1987 and in final form 26 May 1988)

Abstract—An inverse radiation analysis is presented for determining optical thickness and single scattering albedo from the exit intensities for an isotropically scattering slab of finite thickness. The method involves solving the non-linear least square equations constructed from the measured data and the exact solutions. The confidence bounds are developed to assess the accuracy of the inverse solutions. The confidence bounds are useful to determine the possible corrective measures needed to improve the precision of the predictions.

INTRODUCTION

INVERSE analysis of radiative transfer is concerned with the determination of radiative properties from a set of measured radiation quantities. Such a problem has numerous applications in many different areas, including, among others, remote sensing for the atmospheric or aerosol properties [1, 2], temperature measurement in glass manufacturing [3], and experiments for obtaining material properties [4, 5].

A considerable amount of work has been reported for determining single scattering albedo and the scattering phase function from measurements of surface radiation intensities [6–15]. A thorough review of recent literature by McCormick [16–18] reveals that almost all previous inverse analysis requires moments of incident and emerging radiation intensities. Such a requirement necessitates the numerical integration of the angular intensities over the polar angles for the azimuthally symmetric case, and over both the polar and azimuthal angles for azimuthally varying radiation. When intensities are available only in a finite number of directions, the effects of errors involved in the calculation of angular moments on the estimated parameters were demonstrated by Sanchez and McCormick [13]. Oelund and McCormick [15] tried to reduce the errors involved in such integrations by using a split collocation mesh for measurements and cubic splines to interpolate the Gauss–Legendre integration node points. Some investigators [19, 20] assumed that the optical thickness was known, and tried to determine the single scattering albedo by the inverse Monte-Carlo method. Recently, Kamiuto and Seki [21] applied the P_1 approximation to determine the single scattering albedo and the asymmetry factor; but, because of the inaccuracy of the P_1 approximation, predictions were poor for medium-high to low values of albedo.

Here, we present a straightforward approach to determine the optical thickness and the single scattering albedo directly from measured exit intensities, either reflected, transmitted, or both, without a need

for integration over all solid angles. The method involves the solution of non-linear least square equations constructed from the measured data and the exact solution for the exit intensities. Measured data are simulated by adding random errors to the exact solutions of the direct problem, or by rounding the exact solutions to a specific number of digits. To assess the accuracy of predictions, a statistical analysis is made to establish confidence bounds for the inverse solution. Confidence bounds are useful not only for estimating the accuracy of predictions, but also determining whether any corrective measures are needed to improve the precision of predictions.

ANALYSIS

Consider a homogeneous, azimuthally symmetric, absorbing, isotropically scattering, gray, plane-parallel medium of optical thickness τ_0 subjected to isotropic incident radiation at the boundary surfaces $\tau = 0$ and no external incident radiation at $\tau = \tau_0$. The equation of radiative transfer and the boundary conditions are taken as

$$\mu \frac{\partial I(\tau, \mu)}{\partial \tau} + I(\tau, \mu) = \frac{\omega}{2} \int_{-1}^1 I(\tau, \mu') d\mu',$$

$$\text{in } 0 < \tau < \tau_0, -1 \leq \mu \leq 1 \quad (1a)$$

$$I(0, \mu) = 1, \quad \mu > 0 \quad (1b)$$

$$I(\tau_0, -\mu) = 0, \quad \mu > 0. \quad (1c)$$

Here, $I(\tau, \mu)$ is the radiation intensity, τ the optical variable, μ the cosine of the angle between the direction of the radiation intensity and the positive τ -axis, and ω the single scattering albedo. We assume that the exit radiation intensities at the boundary surfaces $\tau = 0$ and τ_0 can be measured experimentally, and we attempt to find the optical thickness, τ_0 , and the single scattering albedo, ω , of the medium by utilizing such experimental data.

The exact solutions of radiation intensities to the

NOMENCLATURE

A_j, B_j	expansion coefficients in equations (2)	Greek symbols	
e_i	normally distributed random number in equation (15)	$\delta \tilde{I}_i$	measured error, $\tilde{I}_i - I_i$
$g_l(\xi)$	Chandrasekhar's polynomials	μ	direction cosine
$H_1(\mu, \xi_j), H_2(\mu, \xi_j)$	functions defined by equations (5)	ξ_i	positive eigenvalues of equation (3)
I	radiation intensity	$[\sigma(\tilde{I}_i)]^2$	variance of the measured intensities
\hat{I}	exact radiation intensity for given estimated $\hat{\omega}$ and $\hat{\tau}_0$	$\sigma(\hat{\omega})$	standard deviation of the estimated single scattering albedo
\tilde{I}	measured radiation intensity	$\sigma(\hat{\tau}_0)$	standard deviation of the estimated optical thickness
\bar{I}	average radiation intensity	τ	optical variable
N	number of measured data	τ_0	optical thickness
S	quantity defined by equation (6)	$\hat{\tau}_0$	estimated optical thickness
X	inverse function defined by equations (8)	ω	single scattering albedo
Y_1, Y_2	functions defined by equations (7).	$\hat{\omega}$	estimated single scattering albedo.

direct problem defined by equations (1) have been given in ref. [22]. The evaluation of this solution at each boundary surface gives

$$I(0, -\mu) = \frac{\omega}{4\pi} \sum_{j=1}^J \xi_j [A_j H_2(\mu, \xi_j) + B_j H_1(\mu, \xi_j)], \quad \mu > 0 \quad (2a)$$

and

$$I(\tau_0, \mu) = e^{-\tau_0/\mu} + \frac{\omega}{4\pi} \sum_{j=1}^J \xi_j [A_j H_1(\mu, \xi_j) + B_j H_2(\mu, \xi_j)], \quad \mu > 0 \quad (2b)$$

for the case of $\omega < 1$, and

$$I(0, -\mu) = \frac{1}{4\pi} [1 - e^{-\tau_0/\mu}] A_J + \frac{1}{4\pi} [\mu(1 - e^{-\tau_0/\mu}) - \tau_0 e^{-\tau_0/\mu}] B_J + \frac{1}{4\pi} \sum_{j=1}^{J-1} \xi_j [A_j H_2(\mu, \xi_j) + B_j H_1(\mu, \xi_j)], \quad \mu > 0 \quad (2c)$$

and

$$I(\tau_0, \mu) = e^{-\tau_0/\mu} + \frac{1}{4\pi} [1 - e^{-\tau_0/\mu}] A_J + \frac{1}{4\pi} [\tau_0 - \mu(1 - e^{-\tau_0/\mu})] B_J + \frac{1}{4\pi} \sum_{j=1}^{J-1} \xi_j [A_j H_1(\mu, \xi_j) + B_j H_2(\mu, \xi_j)], \quad \mu > 0 \quad (2d)$$

for the case of $\omega = 1$.

The $2J$ unknown expansion coefficients, A_j and B_j , in equations (2) are determined by solving $2J$ linear algebraic equations as described in ref. [22], where $J = (M+1)/2$. In addition, M is an odd integer which represents the order of expansion of radiation intensity in terms of the Legendre polynomials, and the ξ_j

are the positive eigenvalues of the eigenvalue problem constructed in the form [23]

$$\left[\frac{l(l-1)}{h_l h_{l-1}} \right] g_{l-2}(\xi) + \frac{1}{h_l} \left[\frac{(l+1)^2}{h_{l+1}} + \frac{l^2}{h_{l-1}} \right] g_l(\xi) + \left[\frac{(l+2)(l+1)}{h_{l+1} h_l} \right] g_{l+2}(\xi) = \xi^2 g_l(\xi) \quad (3)$$

for $l = 0, 2, 4, \dots, M-1$, and h_l are computed from $h_l = 2l+1 - \delta_{0l}$, where δ_{0l} is Kronecker's delta. The functions $g_l(\xi)$ are Chandrasekhar's polynomial determined from the recurrence formula [24]

$$(l+1)g_{l+1}(\xi) = h_l \xi g_l(\xi) - l g_{l-1}(\xi) \quad (4)$$

with $g_0(\xi) = 1$.

The functions $H_1(\mu, \xi_j)$ and $H_2(\mu, \xi_j)$ appearing in equations (2) are defined as

$$H_1(\mu, \xi) = \frac{e^{-\tau_0/\mu} - e^{-\tau_0/\xi_j}}{\mu - \xi_j} \quad (5a)$$

and

$$H_2(\mu, \xi) = \frac{1 - e^{-\tau_0/\mu} - \tau_0/\xi_j}{\mu + \xi_j} \quad (5b)$$

The inverse analysis is performed as follows. Let \tilde{I}_i , $i = 1, 2, \dots, N$, be the measured exit intensities at N polar angles and $\hat{I}_i(\hat{\omega}, \hat{\tau}_0)$ be the exact exit intensities for a given estimated single scattering albedo, $\hat{\omega}$, and optical thickness, $\hat{\tau}_0$, at corresponding polar angles. We wish to minimize the quantity

$$S = \sum_{i=1}^N (\tilde{I}_i - \hat{I}_i(\hat{\omega}, \hat{\tau}_0))^2 \quad (6)$$

such that the values of $\hat{\omega}$ and $\hat{\tau}_0$ yield a minimum for S in equation (6). The quantity S is minimized by imposing the requirements

$$Y_1 \equiv \sum_{i=1}^N \frac{\partial \hat{I}_i(\hat{\omega}, \hat{\tau}_0)}{\partial \hat{\omega}} [\tilde{I}_i - \hat{I}_i(\hat{\omega}, \hat{\tau}_0)] = 0 \quad (7a)$$

and

$$Y_2 \equiv \sum_{i=1}^N \frac{\partial \hat{I}_i(\hat{\omega}, \hat{\tau}_0)}{\partial \hat{\tau}_0} [\tilde{I}_i - \hat{I}_i(\hat{\omega}, \hat{\tau}_0)] = 0. \quad (7b)$$

These non-linear equations are solved by the finite difference Levenberg–Marquardt algorithm [25, 26] and the unknown $\hat{\omega}$ and $\hat{\tau}_0$ are determined.

CONFIDENCE BOUNDS

In order to assess the validity and accuracy of inverse solutions, the confidence bounds are now developed for the predicted parameters. Let X be the inverse function such that

$$\omega = X(I_1, I_2, \dots, I_N) \quad (8a)$$

and

$$\hat{\omega} = X(\tilde{I}_1, \tilde{I}_2, \dots, \tilde{I}_N). \quad (8b)$$

Here, I_i and \tilde{I}_i are the exact and measured exit intensities, respectively, while ω and $\hat{\omega}$ are the exact and estimated single scattering albedo, respectively. The Taylor series expansion of equation (8a) can be written as

$$\begin{aligned} \omega = X(\tilde{I}_1, \tilde{I}_2, \dots, \tilde{I}_N) &- \left[\frac{\partial X(\tilde{I}_1, \tilde{I}_2, \dots, \tilde{I}_N)}{\partial \tilde{I}_1} \delta_{I_1} \right. \\ &+ \frac{\partial X(\tilde{I}_1, \tilde{I}_2, \dots, \tilde{I}_N)}{\partial \tilde{I}_2} \delta_{I_2} + \dots + \frac{\partial X(\tilde{I}_1, \tilde{I}_2, \dots, \tilde{I}_N)}{\partial \tilde{I}_N} \delta_{I_N} \left. \right] \\ &+ [\text{Higher Order Terms}] \quad (9) \end{aligned}$$

with δ_{I_i} being the measured errors with zero mean defined as $\tilde{I}_i - I_i$. We now replace $X(\tilde{I}_1, \tilde{I}_2, \dots, \tilde{I}_N)$ by $\hat{\omega}$, neglect the higher order terms, and rearrange to obtain the standard deviation for $\hat{\omega}$ as

$$\sigma(\hat{\omega}) = \left[\sum_{i=1}^N \left(\frac{\partial \hat{\omega}}{\partial \tilde{I}_i} \right)^2 [\sigma(\tilde{I}_i)]^2 \right]^{1/2}. \quad (10a)$$

Here, $[\sigma(\tilde{I}_i)]^2$ is the variance of the measured intensities \tilde{I}_i , and the measured data \tilde{I}_i are assumed to be independent of each other such that $\sigma(\tilde{I}_i \tilde{I}_k) = 0$, for $j \neq k$.

Analogous to equation (10a), the standard deviation for $\hat{\tau}_0$ is given by

$$\sigma(\hat{\tau}_0) = \left[\sum_{i=1}^N \left(\frac{\partial \hat{\tau}_0}{\partial \tilde{I}_i} \right)^2 [\sigma(\tilde{I}_i)]^2 \right]^{1/2}. \quad (10b)$$

We note that the derivatives $\partial \hat{\omega} / \partial \tilde{I}_i$ and $\partial \hat{\tau}_0 / \partial \tilde{I}_i$ represent the sensitivity coefficients for the solutions $\hat{\omega}$ and $\hat{\tau}_0$ with respect to the measured data \tilde{I}_i . To calculate $\partial \hat{\omega} / \partial \tilde{I}_i$ and $\partial \hat{\tau}_0 / \partial \tilde{I}_i$ we compute the total differentials of Y_1 and Y_2 , defined by equations (7), and rearrange the results in matrix form as

$$\begin{bmatrix} \frac{\partial \hat{\omega}}{\partial \tilde{I}_1} & \frac{\partial \hat{\omega}}{\partial \tilde{I}_2} & \dots & \frac{\partial \hat{\omega}}{\partial \tilde{I}_N} \\ \frac{\partial \hat{\tau}_0}{\partial \tilde{I}_1} & \frac{\partial \hat{\tau}_0}{\partial \tilde{I}_2} & \dots & \frac{\partial \hat{\tau}_0}{\partial \tilde{I}_N} \end{bmatrix} = - \begin{bmatrix} \frac{\partial Y_1}{\partial \hat{\omega}} & \frac{\partial Y_1}{\partial \hat{\tau}_0} \\ \frac{\partial Y_2}{\partial \hat{\omega}} & \frac{\partial Y_2}{\partial \hat{\tau}_0} \end{bmatrix}^{-1} \cdot \begin{bmatrix} \frac{\partial Y_1}{\partial \tilde{I}_1} & \frac{\partial Y_1}{\partial \tilde{I}_2} & \dots & \frac{\partial Y_1}{\partial \tilde{I}_N} \\ \frac{\partial Y_2}{\partial \tilde{I}_1} & \frac{\partial Y_2}{\partial \tilde{I}_2} & \dots & \frac{\partial Y_2}{\partial \tilde{I}_N} \end{bmatrix}. \quad (11)$$

We substitute the definitions of Y_1 and Y_2 into equation (11) and neglect the terms involving higher order derivatives of \tilde{I}_i [27]; then the following expression is obtained for the determination of the derivatives $\partial \hat{\omega} / \partial \tilde{I}_i$ and $\partial \hat{\tau}_0 / \partial \tilde{I}_i$, $i = 1, 2, \dots, N$, in equations (10)

$$\begin{bmatrix} \frac{\partial \hat{\omega}}{\partial \tilde{I}_1} & \frac{\partial \hat{\omega}}{\partial \tilde{I}_2} & \dots & \frac{\partial \hat{\omega}}{\partial \tilde{I}_N} \\ \frac{\partial \hat{\tau}_0}{\partial \tilde{I}_1} & \frac{\partial \hat{\tau}_0}{\partial \tilde{I}_2} & \dots & \frac{\partial \hat{\tau}_0}{\partial \tilde{I}_N} \end{bmatrix} = \begin{bmatrix} \frac{\partial \hat{I}_1}{\partial \hat{\omega}} & \frac{\partial \hat{I}_1}{\partial \hat{\tau}_0} \\ \frac{\partial \hat{I}_2}{\partial \hat{\omega}} & \frac{\partial \hat{I}_2}{\partial \hat{\tau}_0} \\ \vdots & \vdots \\ \frac{\partial \hat{I}_N}{\partial \hat{\omega}} & \frac{\partial \hat{I}_N}{\partial \hat{\tau}_0} \end{bmatrix}^{-1} \cdot \begin{bmatrix} \frac{\partial \hat{I}_1}{\partial \hat{\omega}} & \frac{\partial \hat{I}_1}{\partial \hat{\tau}_0} \\ \frac{\partial \hat{I}_2}{\partial \hat{\omega}} & \frac{\partial \hat{I}_2}{\partial \hat{\tau}_0} \\ \vdots & \vdots \\ \frac{\partial \hat{I}_N}{\partial \hat{\omega}} & \frac{\partial \hat{I}_N}{\partial \hat{\tau}_0} \end{bmatrix} \quad (12)$$

where the derivatives $\partial \hat{I}_i / \partial \hat{\omega}$ and $\partial \hat{I}_i / \partial \hat{\tau}_0$ are calculated by finite differences evaluated at $(\hat{\omega}, \hat{\tau}_0)$.

Since, in an inverse problem, the exact intensities are not known, the variance of measured data, $\sigma(\tilde{I}_i)^2$, cannot be obtained for each \tilde{I}_i . We assume a constant variance for the measured data and replace $[\sigma(\tilde{I}_i)]^2$ by the constant variance, $[\sigma(\tilde{I})]^2$. When equation (12) is substituted into equations (10), the following expression is obtained for the variance of $\hat{\omega}$ and $\hat{\tau}_0$:

$$\begin{bmatrix} [\sigma(\hat{\omega})]^2 \\ [\sigma(\hat{\tau}_0)]^2 \end{bmatrix} = [\sigma(\tilde{I})]^2 \cdot \text{diag} \left[\begin{bmatrix} \sum_{i=1}^N \left(\frac{\partial \hat{I}_i}{\partial \hat{\omega}} \right)^2 & \sum_{i=1}^N \left(\frac{\partial \hat{I}_i}{\partial \hat{\omega}} \right) \left(\frac{\partial \hat{I}_i}{\partial \hat{\tau}_0} \right) \\ \sum_{i=1}^N \left(\frac{\partial \hat{I}_i}{\partial \hat{\tau}_0} \right) \left(\frac{\partial \hat{I}_i}{\partial \hat{\omega}} \right) & \sum_{i=1}^N \left(\frac{\partial \hat{I}_i}{\partial \hat{\tau}_0} \right)^2 \end{bmatrix} \right]^{-1}. \quad (13)$$

The standard deviations $\sigma(\hat{\omega})$ and $\sigma(\hat{\tau}_0)$ are then obtained by taking the square roots of equation (13).

Once the inverse solutions are obtained from the measured data, the derivatives $\partial \hat{I}_i / \partial \hat{\omega}$ and $\partial \hat{I}_i / \partial \hat{\tau}_0$ are calculated by finite differences, and the standard devi-

Table 1. Predicted single scattering albedo, $\hat{\omega}$, and optical thickness, $\hat{\tau}_0$, using exact intensities as the measured data

ω	τ_0	$\hat{\omega}$	Percentage error	τ_0	Percentage error
(a) Results obtained from transmitted intensities					
0.1	0.1	0.100055	0.055250	0.100003	0.003278
0.5	0.1	0.500000	0.000058	0.100000	0.000024
0.9	0.1	0.900001	0.000066	0.100000	0.000060
0.1	1.0	0.100100	0.100043	1.000039	0.003902
0.5	1.0	0.500006	0.001271	1.000004	0.000439
0.9	1.0	0.899996	0.000495	0.999990	0.001029
0.1	2.0	0.099728	0.271637	1.999836	0.008179
0.5	2.0	0.500008	0.001615	2.000011	0.000530
0.9	2.0	0.899997	0.000364	1.999981	0.000967
(b) Results obtained from reflected intensities					
0.1	0.1	0.100000	0.000037	0.100000	0.000060
0.5	0.1	0.500000	0.000075	0.100000	0.000127
0.9	0.1	0.899999	0.000063	0.100000	0.000124
0.1	1.0	0.100000	0.000399	1.000061	0.006120
0.5	1.0	0.499996	0.000833	1.000060	0.005953
0.9	1.0	0.900003	0.000366	0.999979	0.002102
0.1	2.0	0.100006	0.006404	1.991497	0.425146
0.5	2.0	0.500027	0.005435	1.997446	0.127682
0.9	2.0	0.900000	0.000031	1.999991	0.000441

Table 2. Predicted single scattering albedo, $\hat{\omega}$, and optical thickness, $\hat{\tau}_0$, obtained from intensities with measured errors

Error type	ω	τ_0	$\hat{\omega}$	Percentage error	$\hat{\tau}_0$	Percentage error
(a) Results obtained from transmitted intensities						
Random†	0.1	1.0	0.1110	11.000	1.0037	0.370
T4	0.1	1.0	0.0911	8.915	0.9965	0.345
T3	0.1	1.0	0.0938	6.153	0.9974	0.260
T2	0.1	1.0	0.0930	7.043	0.9954	0.460
Random	0.5	1.0	0.4984	0.320	0.9981	0.190
T4	0.5	1.0	0.4997	0.068	0.9997	0.026
T3	0.5	1.0	0.4997	0.057	0.9998	0.021
T2	0.5	1.0	0.4998	0.032	0.9999	0.014
Random	0.9	1.0	0.9061	0.673	1.0161	1.608
T4	0.9	1.0	0.8998	0.019	0.9996	0.039
T3	0.9	1.0	0.8991	0.103	0.9998	0.023
T2	0.9	1.0	0.9072	0.805	1.0146	1.455
(b) Results obtained from reflected intensities						
Random†	0.1	1.0	0.0998	0.200	1.0426	4.260
T4	0.1	1.0	0.1000	0.037	1.0065	0.652
T3	0.1	1.0	0.0999	0.130	1.0109	1.088
T2	0.1	1.0	0.1020	1.951	1.4818	48.181
Random	0.5	1.0	0.5011	0.220	0.9949	0.510
T4	0.5	1.0	0.5000	0.001	1.0003	0.026
T3	0.5	1.0	0.4990	0.202	1.0169	1.686
T2	0.5	1.0	0.4986	0.283	1.0103	1.031
Random	0.9	1.0	0.9026	0.290	0.9794	2.059
T4	0.9	1.0	0.8999	0.009	1.0005	0.050
T3	0.9	1.0	0.8996	0.049	1.0027	0.269
T2	0.9	1.0	0.9013	0.141	0.9944	0.563

† Assumed 5% measured errors at 99% confidence.

ations of $\hat{\omega}$ and $\hat{\tau}_0$ are readily obtained from equation (13) to establish the confidence bounds for the estimated parameters. For example, for normally distributed measured errors, the 99% confidence bounds about $\hat{\omega}$ and $\hat{\tau}_0$ are given, respectively, by

$$\hat{\omega} \pm 2.576\sigma(\hat{\omega}) \quad (14a)$$

and

$$\hat{\tau}_0 \pm 2.576\sigma(\hat{\tau}_0) \quad (14b)$$

where 2.576 arises from the fact that 99% of a normally distributed population is contained within ± 2.576 standard deviations of the mean.

RESULTS AND DISCUSSION

Numerical results are now presented to illustrate the applications of the foregoing inverse analysis for determining $\hat{\omega}$ and $\hat{\tau}_0$ and the confidence bounds. A FORTRAN program from the IMSL program package [26] was used to solve the non-linear least square equation, equation (6), satisfying the requirements given by equations (7) for the unknown parameters $\hat{\omega}$ and $\hat{\tau}_0$.

Tables 1(a) and (b) demonstrate the determination of $\hat{\omega}$ and $\hat{\tau}_0$ by using the exact transmitted and reflected intensities, respectively. The exit intensities $I_i^-(0)$ and $I_i^+(\tau_0)$, $i = 1, 2, \dots, 19$, were calculated from equations (2) for various combinations of $\omega = 0.1, 0.5$, and 0.9 and $\tau_0 = 0.1, 1.0$, and 2.0 by dividing $0 \leq \theta \leq 90$ into 18 equal intervals. The estimated values of $\hat{\omega}$ and $\hat{\tau}_0$ are found to be in excellent agreement with the exact ω and τ_0 for all cases as shown in Table 1. The worst case for $\hat{\omega}$ occurred with $\omega = 0.1$ and $\tau_0 = 2.0$, when the transmitted intensities were used as the measured data; the relative error was 0.27%. The worst $\hat{\tau}_0$ occurred with $\omega = 0.1$ and $\tau_0 = 2.0$, when the reflected intensities were used as measured data; the relative error was 0.43%.

To demonstrate the effects of measurement errors on the predicted parameters, we considered two types of errors: the truncation error and the random error. The measured exit intensities with truncation error were obtained by rounding the exact solutions to a specific number of digits, while the measured exit intensities with random error were obtained by adding normally distributed errors into exact solutions as

$$\tilde{I}_i = I_i + e_i \sigma(\tilde{I}), \quad i = 1, 2, \dots, N. \quad (15)$$

Here, $0 < e_i < 1$ is the normally distributed random number with unit standard deviation and zero mean. The standard deviation of measured intensities $\sigma(\tilde{I})$, for a 5% measured error at 99% confidence, is determined as

$$\sigma(\tilde{I}) = \frac{\bar{I} \times 5\%}{2.576} \quad (16)$$

where \bar{I} is the average exit intensities and 2.576 arises from the fact that 99% of a normally distributed

population is contained within ± 2.576 standard deviations of the mean.

Tables 2(a) and (b) show the effects of measurement errors on the estimated $\hat{\omega}$ and $\hat{\tau}_0$ obtained from the transmitted and reflected intensities, respectively. Three values of single scattering albedo considered include $\omega = 0.1, 0.5$, and 0.9 and the optical thickness is taken as $\tau_0 = 1.0$. The error types T4, T3, and T2 represent the measured intensities obtained by rounding the exact solutions to 4, 3, and 2 significant digits, respectively. The estimated values of $\hat{\omega}$ and $\hat{\tau}_0$ were within 2% for the cases of $\omega = 0.5$ and 0.9 . For the case of $\omega = 0.1$, the errors involved in the inverse solutions for $\hat{\omega}$ varied from 6 to 11% when the transmitted intensities were used as the measured data, while the errors for $\hat{\tau}_0$ varied from 0.6 to 49% when the reflected intensities were used as the measured data. The results given in Tables 2(a) and (b) suggest that, for small values of ω , the optical thickness should be determined from the transmitted intensities while the single scattering albedo should be determined from the reflected intensities.

Figures 1 and 2 show the confidence bounds about $\hat{\tau}_0$ and $\hat{\omega}$ for the case of $\omega = 0.5$ and 0.1 , respectively, with optical thickness taken as $\tau_0 = 1.0$. The measured

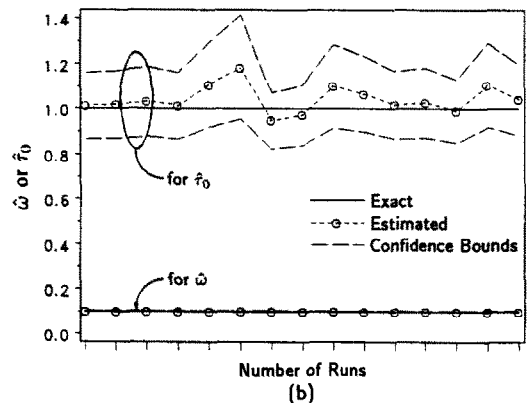
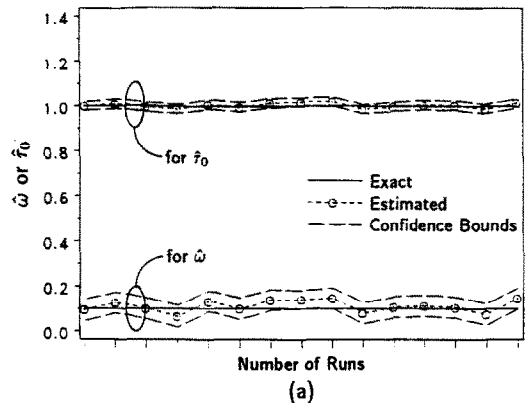


FIG. 1. Confidence bounds about $\hat{\omega}$ and $\hat{\tau}_0$ using: (a) transmitted, (b) reflected intensities as measured data for the case of $\omega = 0.1$ and $\tau_0 = 1.0$.

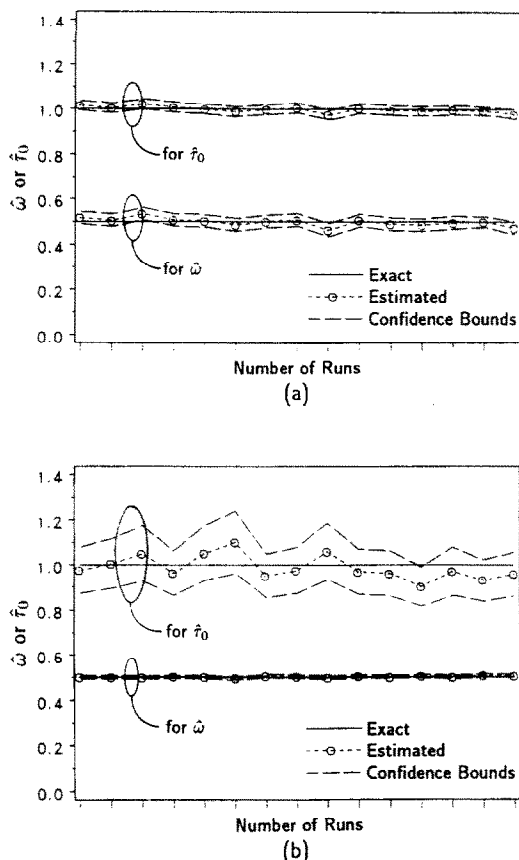


FIG. 2. Confidence bounds about $\hat{\omega}$ and $\hat{\tau}_0$ using: (a) transmitted, (b) reflected intensities as measured data for the case of $\omega = 0.5$ and $\tau_0 = 1.0$.

errors introduced in the intensities are 5% normally distributed random errors at 99% confidence. Different sets of random numbers e_i were used to repeat the inverse calculations. As expected, Figs. 1 and 2 show that the confidence bounds about $\hat{\omega}$ and $\hat{\tau}_0$ covered the exact values of ω and τ_0 except at a few data points. Figures 1(a) and 2(a) show that the confidence bounds are narrower for $\hat{\tau}_0$ when using the transmitted intensities as the measured data, while Figs. 1(b) and 2(b) show that the confidence bounds are narrower for $\hat{\omega}$ when using the reflected intensities as the measured data. Such results conclude that, for small values of ω , it is preferable to determine the optical thickness from the transmitted exit intensities and the single scattering albedo from the reflected exit intensities.

Acknowledgement—The support from the NATO Grant No. 85-0334 is gratefully acknowledged.

REFERENCES

1. E. A. Ustinov, The inverse problem of multi-scattering theory and the interpolation of measurements of scattered radiation in the cloud layer of Venus, *Cosmic Res.* **15**(5), 667–672 (1977).
2. J. Freund, Aerosol single scattering albedo in the Arctic, determined from ground-based nonspecial solar irradiance measurements, *J. Atmos. Sci.* **40**(11), 2724–2731 (1983).
3. R. Van Laethem, M. Leger and E. Plumet, Temperature measurement of glass by radiation analysis, *J. Am. Ceram. Soc.* **44**, 321–332 (1961).
4. J. A. Roux and A. M. Smith, Determination of radiative properties from transport theory and experimental data, AIAA 16th Thermophysics Conf., Palo Alto, California, 23–25 June (1981).
5. J. F. Sacadura, G. Uny and A. Venet, Models and experiments for radiation parameter estimation of absorbing, emitting, and anisotropically scattering media, *Proc. 8th Heat Transfer Conf.*, Vol. 2, pp. 565–570 (1986).
6. C. E. Siewert, A new approach to the inverse problem, *J. Math. Phys.* **19**, 2619–2621 (1978).
7. M. Kanal and J. A. Davies, A multidimensional inverse problem in transport theory, *Transp. Theory Stat. Phys.* **8**, 99–115 (1979).
8. C. E. Siewert, On the inverse problem for a three-term phase function, *J. Quant. Spectrosc. Radiat. Transfer* **22**, 441–446 (1979).
9. N. J. McCormick, Transport scattering coefficients from reflection and transmission measurements, *J. Math. Phys.* **20**, 1504–1507 (1979).
10. W. L. Dunn and J. R. Maiorino, On the numerical characteristics of an inverse solution for three-term radiative transfer, *J. Quant. Spectrosc. Radiat. Transfer* **24**, 203–209 (1980).
11. N. J. McCormick and R. Sanchez, Inverse problem transport calculations for anisotropic scattering coefficients, *J. Math. Phys.* **22**, 199–208 (1981).
12. R. Sanchez and N. J. McCormick, General solutions to inverse transport problems, *J. Math. Phys.* **22**, 847–855 (1981).
13. R. Sanchez and N. J. McCormick, Numerical evaluation of optical single-scattering properties using multiple-scattering transport methods, *J. Quant. Spectrosc. Radiat. Transfer* **28**, 169–184 (1982).
14. E. W. Larsen, Solution of multidimensional inverse transport problems, *J. Math. Phys.* **25**, 131–135 (1984).
15. J. C. Oelund and N. J. McCormick, Sensitivity of multiple-scattering inverse transport methods to measurement errors, *J. Opt. Soc. Am.* **A2**, 1972–1978 (1985).
16. N. J. McCormick, A critique of inverse solutions to slab geometry transport problems, *Prog. Nucl. Energy* **8**, 235–245 (1981).
17. N. J. McCormick, Recent developments in inverse scattering transport methods, *Transp. Theory Stat. Phys.* **13**, 15–28 (1984).
18. N. J. McCormick, Methods for solving inverse problems for radiation transport—an update, *Transp. Theory Stat. Phys.* **15**, 759–772 (1986).
19. W. L. Dunn, Inverse Monte Carlo analysis, *J. Comput. Phys.* **41**, 154–166 (1981).
20. W. L. Dunn, Inverse Monte Carlo solutions for radiative transfer in inhomogeneous media, *J. Quant. Spectrosc. Radiat. Transfer* **29**, 19–26 (1983).
21. K. Kamiuto and J. Seki, Study of the P_1 approximation in an inverse scattering problem, *J. Quant. Spectrosc. Radiat. Transfer* **37**, 455–459 (1987).
22. S. T. Thynell and M. N. Özışık, A new efficient method of solution to radiation transfer in absorbing, emitting, isotropically scattering, homogeneous, finite or semi-infinite, plane-parallel media, *J. Quant. Spectrosc. Radiat. Transfer* **36**, 39–50 (1986).
23. M. Benassi, R. M. Cotta and C. E. Siewert, The P_N method for radiative transfer problems with reflective boundary conditions, *J. Quant. Spectrosc. Radiat. Transfer* **30**, 547–553 (1983).

24. S. Chandrasekhar, *Radiative Transfer*. Dover, New York (1960).
25. K. M. Brown and J. E. Dennis, Jr., Derivative free analogues of the Levenberg-Marquardt and Gauss algorithms for nonlinear least squares approximation, *Numer. Math.* **18**, 289–297 (1972).
26. *IMSL Library*, Edn 9, NBC Building, 7500 Ballaire Blvd., Houston, Texas (1982).
27. A. R. Gallant, *Nonlinear Statistical Models*, pp. 16–17, 259–260. Wiley, New York (1987).

UN PROBLEME DE RAYONNEMENT INVERSE

Résumé—Une étude de rayonnement inverse est faite pour déterminer l'épaisseur optique et l'albedo de diffusion à partir des intensités sortant d'une lame à diffusion isotrope et d'épaisseur finie. La méthode résout les équations non linéaires de moindre carré, construites à partir des mesures et des solutions exactes. Les limites de confiance sont développées pour fixer la précision des solutions inverses. Ces limites de confiance sont utiles pour déterminer les corrections possibles, pour améliorer la précision des prévisions.

EIN INVERSES STRAHLUNGSPROBLEM

Zusammenfassung—Es wird ein inverses Verfahren der Strahlungsberechnung vorgestellt, mit dessen Hilfe aus der Austrittsintensität an einer isotrop streuenden dünnen Scheibe optische Dicke und Albedo bestimmt werden können. Das Verfahren enthält die Lösung der nichtlinearen Regressionsgleichungen, die die Meßdaten mit den berechneten Werten verknüpfen. Um die Genauigkeit der inversen Lösungen abzuschätzen, werden die Vertrauensgrenzen bestimmt. Diese werden auch dazu verwendet, mögliche Korrekturgrößen zu bestimmen, mit deren Hilfe die Genauigkeit der Berechnung verbessert werden kann.

ОБРАТНАЯ ЗАДАЧА ИЗЛУЧЕНИЯ

Аннотация—Рассмотрена обратная задача по определению оптической толщины и альbedo единичного рассеяния по входной интенсивности при рассеянии на изотропной пластине конечной толщины. Подход включает решение нелинейных уравнений методом наименьших квадратов, построенных по экспериментальным данным и точным решениям. Для оценки точности обратных решений определены границы достоверности метода, на основании которых вносились необходимые поправки для повышения точности расчетов.